



Vertical distribution of zooplankton groups, with an emphasis on fish larvae, in the oxygen minimum zone off southern México (December 2020)

L. Sánchez-Velasco ^{a,*}, F.J. García-De León ^b, E.D. Ruvalcada-Aroche ^c, E. Beier ^c, V.M. Godínez ^d, S.P.A. Jiménez-Rosenberg ^e, E.D. Sánchez-Pérez ^f, F. Contreras-Catala ^c, A. Mnich ^g, N. Verma ^g, M. Altabet ^g

^a Instituto Politécnico Nacional-Centro Interdisciplinario de Ciencias Marinas, Departamento de Oceanología, Av. Instituto Politécnico Nacional S/n, Col. Playa Palo de Santa Rita, La Paz 23096, BCS, Mexico

^b Laboratorio de Genética para la Conservación, Centro de Investigaciones Biológicas del Noroeste, Av. Instituto Politécnico Nacional S/n, Col. Playa Palo de Santa Rita, La Paz 23096, BCS, Mexico

^c Centro de Investigación Científica y de Educación Superior de Ensenada (CICESE), Unidad La Paz, Laboratorio de Macroecología Marina, Miraflorres No. 334, Col. Bella Vista La Paz, La Paz 23050, BCS, Mexico

^d Centro de Investigación Científica y de Educación Superior de Ensenada, Baja California (CICESE), Departamento de Oceanografía Física, Carretera Ensenada Tijuana No. 3918, Zona Playitas, Ensenada 22860, BC, Mexico

^e Instituto Politécnico Nacional-Centro Interdisciplinario de Ciencias Marinas, Departamento de Plancton y Ecología Marina, Av. Instituto Politécnico Nacional S/n, Col. Playa Palo de Santa Rita, La Paz 23096, BCS, Mexico

^f CONACyT-Instituto Politécnico Nacional-Centro Interdisciplinario de Ciencias Marinas, Departamento de Plancton y Ecología Marina, Av. Instituto Politécnico Nacional S/n, Col. Playa Palo de Santa Rita, La Paz 23096, BCS, Mexico

^g University of Massachusetts Dartmouth, School for Marine Science and Technology, Department of Estuarine and Ocean Sciences, 706 S Rodney French Blvd, New Bedford, MA 02744, United States of America

ARTICLE INFO

Keywords:

Zooplankton biomass

Fish larvae

Copepods

Water masses

Oxygen minimum zone

Northeastern Pacific Ocean

ABSTRACT

The distribution of zooplankton groups, with an emphasis on fish larvae, in the Oxygen Minimum Zone off southern Mexico (December 2020) was analyzed. A hydrographic section of five sampling stations was made in the confluence of Transitional Water and Tropical Surface Waters. In each station, horizontal zooplankton trawls on three different dissolved oxygen conditions (~ 100 , < 44 and $< 4.4 \mu\text{mol kg}^{-1}$) were carried out by a MOCNESS net (333 μm). The $100 \mu\text{mol kg}^{-1}$ oxypleth (oxic condition) was ~ 60 m depth along the section, but the $4.4 \mu\text{mol kg}^{-1}$ oxypleth (suboxic) rose southward from Transitional Water (~ 150 m) to Tropical Surface Water (~ 90 m), approaching the well oxygenated layer. The distribution of the zooplankton biomass, and the most abundant zooplankton groups (e.g. copepods, chaetognaths, ostracods, euphausiids) and fish larvae showed statistically significant differences ($P < 0.01$) between the oxic ($100 \mu\text{mol kg}^{-1}$) and the deeper suboxic conditions. The larvae of typically dominant fish species such as the bathypelagic *Vinciguerria lucetia*, *Diogenichthys laternatus*, *Diaphus pacificus* and *Cubiceps pauciradiatus*, were present only in the oxygenated depths in the Transitional Water, and were almost absent from all depths in the Tropical Surface Water, where the oxycline shoaled. These differences in larval fish abundance were found despite little change in chlorophyll *a* concentration (relative units "r.u.") along the sections, indicating that the oxycline is a limiting factor for the fish larvae. The fish larvae results contrast with previous observations from the mouth of the Gulf of California, where some species have distributions independent of water column dissolved oxygen conditions, probably as a consequence of coastal processes. Overall, our results show that even within the OMZ, variations in oxycline depth have biological implications, particularly on meroplanktonic organisms.

1. Introduction

Oxygenation in the ocean is temporally and spatially variable and is

controlled by physical factors like ventilation as well as biotic factors such as photosynthesis and respiration. Oxygen minimum zones (OMZs), where dissolved oxygen can reach undetectable levels at

* Corresponding author.

E-mail address: lsvelasc@ipn.mx (L. Sánchez-Velasco).



relatively shallow depths (~ 40 to 300 m), are found in regions of high primary productivity, where microbial respiration is high below the euphotic zone and the deep circulation derived from polar regions is sluggish (Stramma et al., 2008; Schmidtko et al., 2017; Breitburg et al., 2018). There is no consensus on the oxygen threshold defining an OMZ, but it has been reported that when oxygen concentrations drop below $44 \mu\text{mol kg}^{-1}$ the pelagic organisms may become stressed (so-called hypoxic conditions); and when the oxygen concentrations fall below $4.4 \mu\text{mol kg}^{-1}$ (suboxic conditions) mortality may increase (Diaz and Rosenberg, 2008; Wishner et al., 2013; Gallo and Levin, 2016; Sánchez-Velasco et al., 2017).

Large-scale expansion of OMZs over the past 50 years poses a challenge for predicting impacts on tropical pelagic ecosystems, which are characterized by high species richness (Fernandez-Alamo and Farber-Lorda, 2006; Wishner et al., 2018; Wishner et al., 2020) and abundance of commercially important species (Chávez et al., 2003; Prince and Goodyear, 2006; Ruvalcaba-Aroche et al., 2020). Possible consequences of OMZ expansion include shoaling of the upper oxycline and thinning of the near-surface, well-oxygenated layer where most pelagic organisms, from zooplankton to top predators inhabit (Fernandez-Alamo and Farber-Lorda, 2006; Prince and Goodyear, 2006; Wishner et al., 2020). Therefore, OMZ expansion will likely change organism distributions and lead to behavioral and physiological adaptations (Levin, 2002; Koslow et al., 2011; Sánchez-Velasco et al., 2019).

The OMZ in the eastern tropical Pacific off Mexico is globally the largest OMZ, stretching from the Mexican ($\sim 20^\circ \text{N}$) to Chilean ($\sim 20^\circ \text{S}$) coasts, and extending ocean-ward to 180°E (Stramma et al., 2008; Schmidtko et al., 2017; Breitburg et al., 2018). Due to its large areal extent, it is one of the least studied especially with respect to its physics and biology. Here we focus on the region off southern Mexico (south of 18°N) whose circulation is dominated by two main oceanographic features. The thermocline basin off Tehuantepec induces an anticyclonic circulation in the surface ~ 100 m, with equatorward flow in the coastal area (Wyrtki, 1966; Kessler, 2006). Below this feature, the Mexican Coastal Current flows poleward from the Gulf of Tehuantepec to the entrance of the Gulf of California. During late spring and summer this coastal current is present at the surface in a thin coastal band of ~ 150 km width (Lavín et al., 2006; Gómez-Valdivia et al., 2015). Tropical Surface Water and Transitional Water are present in the area, and below them, the low O_2 Subtropical Subsurface Water ($< 44 \mu\text{mol kg}^{-1}$; Cepeda-Morales et al., 2013; Stramma et al., 2010; Sánchez-Velasco et al., 2019) occupies the vertical extent of the OMZ between ~ 80 m and ~ 600 m depth (Fiedler and Talley, 2006; Stramma et al., 2010; Portela et al., 2016).

Longhurst (1985) published one of the most extensive studies of the vertical distribution of zooplankton in the Costa Rica Dome ($\sim 10^\circ \text{N}$, 93.4°W), an area included in the OMZ of the Pacific Ocean. The author found that most of the zooplankton, including fish larvae, dwelled in the thermocline during both day and night and had distributions that varied with trophic status. While most of the herbivores were found in the thermocline, carnivores were distributed more evenly throughout the water column. Contrasting observations were made by Wishner et al. (2013, 2020) in their comparative study of zooplankton distribution in the Tehuantepec Basin and Costa Rica Dome in relation to dissolved oxygen gradients. These authors showed that independent of OMZ thickness and depth, the OMZ was a depth region where all zooplankton species were almost absent, concluding that vertical expansion of the OMZ would likely impact zooplankton life cycles overall. However, these authors did not consider the influence of O_2 as a limiting factor in fish larvae distributions.

In the northern section of the OMZ off Mexico (north $\sim 18^\circ \text{N}$), from the Gulf of California entrance to off Cabo Corrientes, recent zooplankton studies have included a focus on larval fish. These studies found the highest zooplankton biomass in the oxygenated levels (surface mixed layer and oxycline) as expected. However, fish larvae showed contrasting vertical distributions with species like *Vinciguerria lucetia*

and *Auxis* spp. preferring well-oxygenated levels, while species like *Bregmaceros bathymaster* and *Diogenichthys laternatus* were found at hypoxic and suboxic levels (Davies et al., 2015; Sánchez-Velasco et al., 2017, 2019).

Faced with future deoxygenation of the oceans and knowing that zooplankton are the base of the heterotrophic food web, it is extremely important to know their current distribution and abundance in the water column in relation to oxygen gradients. It is predicted that deoxygenation will reduce favorable, well-oxygenated habitat for zooplankton. The aim of this study is to improve the understanding of the vertical distribution of zooplankton, with an emphasis on fish larvae, in relation to O_2 in the OMZ off southern Mexico where the Tropical Surface Water and Transitional Water converge.

2. Methods

2.1. Sampling strategy and data acquisition

A transect of physical and biological sampling stations was conducted on board R/V Sally Ride (SR2011, Scripps Institution) from December 21 to January 1st, 2020, in the Oxygen Minimum zone off southern Mexico (Fig. 1).

In order to create a synoptic vision of the environmental conditions during the cruise, composite images of Sea Surface Temperature (SST) and Chlorophyll *a* (CHL) of the Moderate-Resolution Imaging Spectroradiometer (MODIS) of the satellite AQUA were downloaded from <https://coastwatch.pfeg.noaa.gov/erddap/index.html>. The data had a $4 \times 4 \text{ km}$ pixel size. In addition, Sea Level Anomaly (SLA) and surface geostrophic current data produced by SSALT/DUACS and distributed by the CNES-Copernicus were downloaded from <https://resources.marine.copernicus.eu>.

The transect included 5 sampling stations located from 17°N , 107°W to 16°N , 106°W . Zooplankton sampling of each station took place at night except for one station where daytime sampling also took place (See Fig. 1, station with a red cross).

At each sampling station, vertical profiles of temperature and conductivity were made in the upper 1000 m with a Sea-Bird 911plus CTD, which was also equipped with dissolved oxygen and fluorescence sensors recently calibrated at Scripps Institution of Oceanography. The data were processed using the manufacturer's software and averaged to 1 dbar (Godínez et al., 2010). Absolute Salinity (S_A , g kg^{-1}) and Conservative Temperature (Θ , $^\circ\text{C}$) were calculated from in situ temperature and practical salinity with the TEOS-10 (Thermodynamic Equation of Seawater-2010) software which was downloaded from <http://www.TEOS-10.org> (IOC et al., 2010; Pawlowicz et al., 2010).

Zooplankton samples were collected using a 1 m^2 MOCNESS which incorporated a Sea-Bird SBE 911plus CTD, with 280 cm long nets, and 333 mesh size (Wiebe et al., 1985a; Wiebe et al., 1985b). In each one of the five-sampling stations, the MOCNESS was deployed with 3 closed nets. Then, three horizontal samples by deployment were obtained. Each horizontal tow had a duration of approximately 10 min at a speed of 1.5 to 2 knots. After an analysis of the CTD vertical profiles previous to each zooplankton sampling station (e.g. Davies et al., 2015; Sánchez-Velasco et al., 2017, 2019), the depth of the three horizontal samplings was decided on the basis of dissolved oxygen gradient in the water column (e.g. Wishner et al., 2013; Wishner et al., 2018; Sánchez-Velasco et al., 2019). The first sample was obtained in suboxic conditions (~ 300 m depth; $\leq 4 \mu\text{mol kg}^{-1}$). The second was obtained below the oxycline (~ 100 m depth; $\geq 44 \mu\text{mol kg}^{-1}$), and the third one was in the oxic conditions (~ 50 m depth; $> 90 \mu\text{mol kg}^{-1}$). This sampling strategy allowed us to evaluate the limitation of dissolved oxygen in the metabolism of zooplankton organisms and their ability to adapt to different oxygen concentrations (e.g. Levin, 2002; Gallo and Levin, 2016).

The filtered volumes (m^3) and the ranges of depth (m) and dissolved oxygen ($\mu\text{mol kg}^{-1}$) of each horizontal tow were shown in the Supplementary Material 1. The variability of dissolved oxygen concentrations

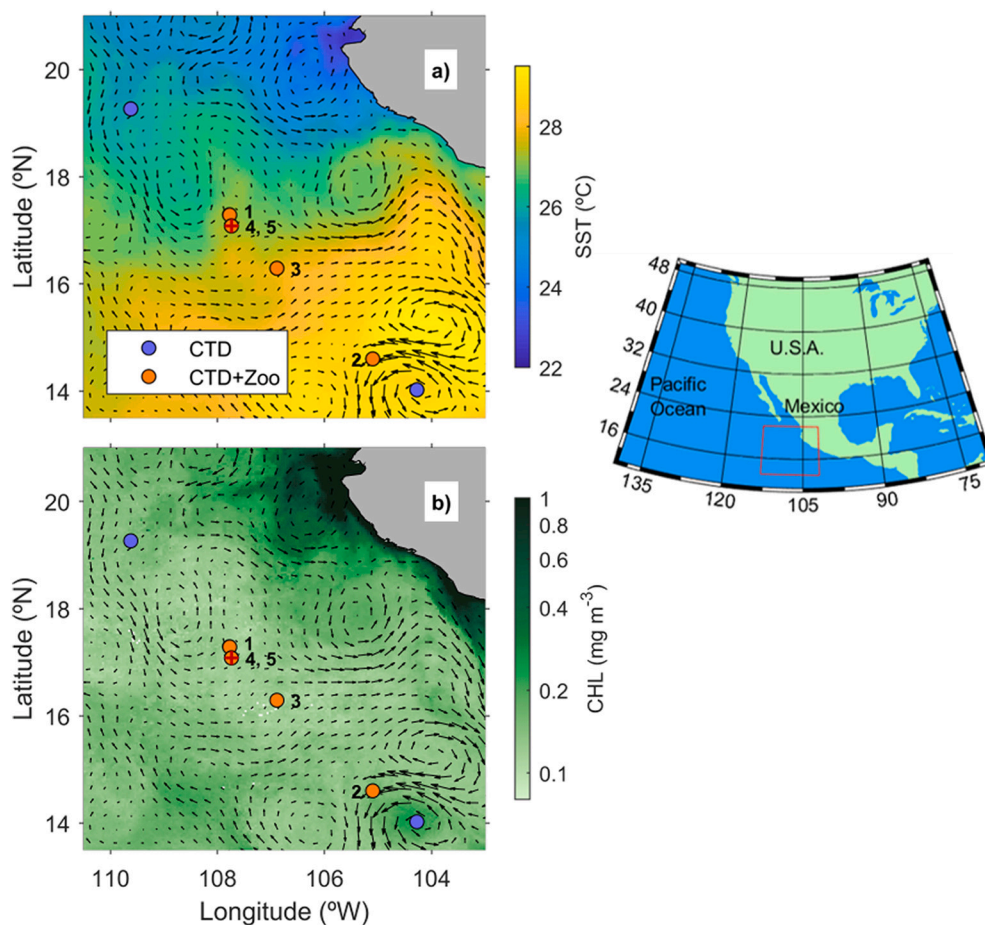


Fig. 1. Location of the study area and sampling stations. Orange dots, mark stations where CTD and zooplankton casts were made, and blue dots mark CTD casts only. All the stations were during night, except the station marked in with a red cross. a) Sea Surface Temperature (SST) and b) Chlorophyll *a* (CHL) imagery from the Moderate-Resolution Imaging Spectroradiometer (MODIS) of the satellite AQUA. Data are composites of daily images from 21 to 30 December 2020, at 4×4 km pixel resolution (<https://coastwatch.pfeg.noaa.gov/erddap/index.html>). Surface geostrophic currents from SSALTO/DUACS and CNES-Copernicus (<https://resources.marine.copernicus.eu>). (For interpretation of the references to colour in this figure legend, the reader is referred to the web version of this article.)

observed during the two deep tows was $<1.3 \mu\text{mol Kg}^{-1}$, and during the oxic tows was $<26 \mu\text{mol Kg}^{-1}$.

A microcomputer system interfaced to the deck unit calculated volume filtered by each net (Supplementary Material 1) and the data were printed out and stored on disc (Wiebe et al., 1985a, 1985b). On deck, nets were rinsed with filtered seawater (Smith and Richardson, 1979), and whole samples were preserved at 96% ethanol, with alcohol replacement at 48 h. for subsequent genetic analysis (not included in this manuscript).

In the laboratory, zooplankton biomass (biolume) was estimated with the displacement volume method (Kramer et al., 1972) and standardized to mL per 1000 m³. Zooplankton species were identified to taxonomic group (e.g., Boltovskoy, 1981; Palomares-García et al., 1998; Suárez-Morales et al., 2000) and counted under a stereoscopic microscope. The entirety of each zooplankton sample was analyzed due to the low zooplankton biomass, characteristic of the open ocean, with the exception of abundant copepods. Copepods were subsampled with a Stempel pipette of 10 mL, from an initial sample volume of 100 mL.

Fish larvae were the only zooplankton group identified until the highest taxonomic category possible. Taxonomic identification was performed primarily according to Moser (1996). The zooplankton groups and the fish larvae were standardized to organism per 1000 m³.

2.2. Statistical analysis

A Kruskal-Wallis multiple comparison test was used to assess the statistical significance of zooplankton biomass (biolume), zooplankton groups, and total fish larvae among different hauls (Daniel, 2008). When the null hypothesis was rejected, a Mann-Whitney test was performed to establish whether significant differences existed between

tows (Sokal and Rohlf, 1985). Fish larvae species were sorted as Dominant (values of relative abundance and frequency of appearance are greater than the arithmetic mean), Constant (relative abundance does not exceed the average value), Occasional (frequency of appearance lower than average), or Rare (relative abundances and frequencies below their respective arithmetic means) according to the Olmstead-Tukey analysis (Sokal and Rohlf, 1985).

Canonical Correspondence Analyses (Ter Braak, 1986) was performed to determine the relationships between the abundance zooplankton groups and environmental variables. Before conducting the analysis, the abundances were fourth-root transformed to homogenize the variance. The matrix of environmental values included average Conservative Temperature (Θ , °C), Absolute Salinity (SA, g kg⁻¹), dissolved oxygen ($\mu\text{mol kg}^{-1}$) and chlorophyll *a* (relative units “r.u.”).

3. Results

3.1. Synoptic hydrography

Along the transect, sea surface temperature increased from NW (~24 °C) to SE (~29 °C). The zooplankton sampling stations encompassed part of this gradient from ~27 °C to ~29 °C (Fig. 1a). CHL images showed mostly oligotrophic conditions ($< 0.5 \text{ mg m}^{-3}$), in the area where sampling stations were located. Nearby coastal areas had CHL values up to 2 mg m^{-3} , with some filaments of high CHL water extending from coastal waters out to the open ocean as a consequence of mesoscale circulation that dominated the region (Fig. 1b). The southern sampling stations were in the margin of a cyclonic circulation field.

The Θ -SA diagram (Fig. 2) showed the presence of both Tropical Surface Water and Transitional Water above the 25 kg m^{-3} isopycnal

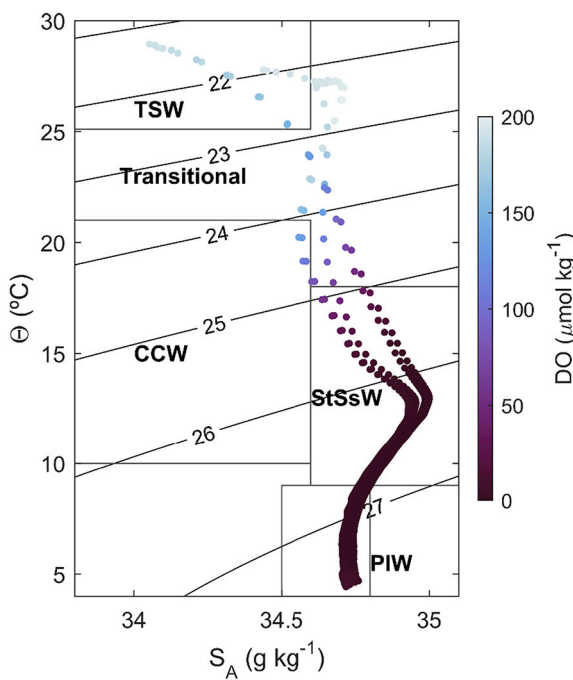


Fig. 2. Water masses in the oxygen minimum zone off southern Mexico (December 2020). (Θ , $^{\circ}\text{C}$), Conservative Temperature. (SA , g kg^{-1}), Absolute Salinity. The water mass limits are according to Portela et al. (2016). Colour bar represents the dissolved oxygen concentration ($\mu\text{mol kg}^{-1}$). TSW, Tropical Surface Water; CCW, California Current Water; StSsW, Subtropical Subsurface Water; PIW, Pacific Intermediate Water.

with dissolved oxygen concentrations $>44 \mu\text{mol kg}^{-1}$. Below this isopycnal were Subtropical Subsurface Water and Pacific Intermediate Water, with dissolved oxygen concentrations $<44 \mu\text{mol kg}^{-1}$ but with suboxic conditions in most of their range.

Sections of temperature, salinity, dissolved oxygen and chlorophyll *a* from surface to 300 m depth are shown in Fig. 3. A warm surface layer (27°C) down to ~ 40 m depth was observed along the entire transect (Fig. 3b), with slightly lower temperatures at the northern station. The thermocline was around ~ 50 m depth and below this temperature decreased from $\sim 15^{\circ}\text{C}$ at 100 m to $\sim 11^{\circ}\text{C}$ at 300 m depth.

A near-surface salinity front was also observed along the section (Fig. 3b). In the SE, a tongue of low salinity ($< 34.4 \text{ g kg}^{-1}$) occurred above 50 m depth showing the presence of fresher water over-riding saltier water below. The 34.8 g kg^{-1} isohaline increased in depth from SE to NW possibly as a consequence of water mass confluence.

The dissolved oxygen distribution (Fig. 3c) showed a well-oxygenated layer over the oxycline from the 60 m depth to surface just above the $100 \mu\text{mol kg}^{-1}$ oxypleth depth along the section. Under the $100 \mu\text{mol kg}^{-1}$ oxypleth, the $4.4 \mu\text{mol kg}^{-1}$ oxypleth deepened from SE (~ 100 m depth) to NW (~ 150 m depth) following the 34.8 g kg^{-1} isohaline. Values $<4.4 \mu\text{mol kg}^{-1}$ were present to at least 300 m depth.

The vertical distribution of chlorophyll *a* (r.u.) (Fig. 3d) showed maximum concentrations (> 0.05 r.u.) around the thermocline at ~ 50 m depth, with higher values in the SE portion of the transect (> 1 r.u.). A second fluorescence maxima was observed in suboxic conditions along the transect at ~ 130 m.

3.2. Zooplankton biomass and dominant groups

Zooplankton biomass values ranged from 0.1 to 48 mL per 1000 m^3 . There were statistically significant differences ($P < 0.01$) (Table 1) in vertical distribution (Fig. 4) among tows, with greater zooplankton biomass along the $100 \mu\text{mol kg}^{-1}$ oxypleth in the oxic conditions. The greatest zooplankton biomass was observed at the NW sampling station,

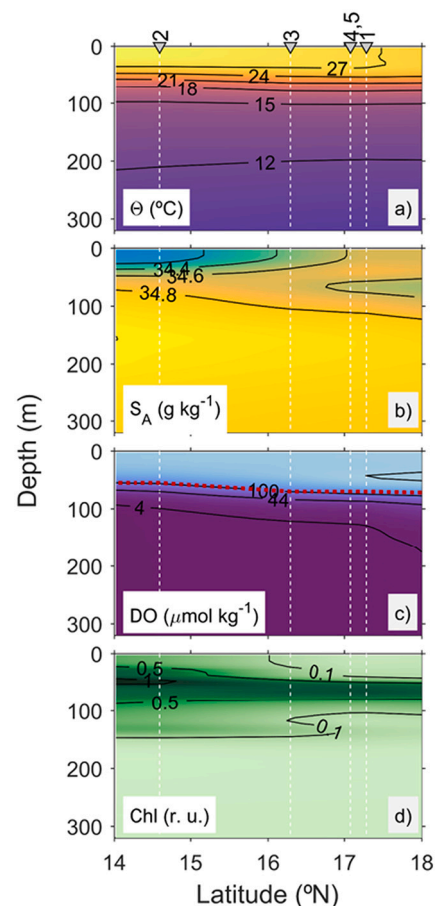


Fig. 3. Vertical distribution of hydrographic conditions along the section shown in Fig. 1. Grey triangles indicate sampling stations. a) Conservative temperature (Θ , $^{\circ}\text{C}$), b) absolute salinity (SA , g kg^{-1}), c) dissolved oxygen (DO, $\mu\text{mol kg}^{-1}$) where the red line represents the oxycline, and d) chlorophyll *a* (Chl, r.u.). (For interpretation of the references to colour in this figure legend, the reader is referred to the web version of this article.)

which coincided with relatively high CHL concentration (r.u.).

Forty-three thousand three hundred fifty organisms were counted in the zooplankton samples. Twenty-seven taxonomic groups were identified (Table 2). The most abundant and representative groups of the holoplankton were copepods (84% of the total abundance), chaetognaths (5.3%), ostracods (2%), pteropods (1.3%), euphausiids (1.6%), appendicularians (0.7%) and amphipods (1%). The fish larvae, meroplanktonic organisms, represented about $\sim 0.2\%$.

These eight taxonomic groups all had maximum concentrations at the $100 \mu\text{mol kg}^{-1}$ oxypleth trawl, with a drastic decline in abundance at the lower O_2 concentrations (Fig. 5). Statistically significant differences ($P < 0.01$) were apparent in all cases between the surface with well-oxygenated waters and the deepest level with suboxic waters (Table 2). Significant differences ($P < 0.01$) were also detected in chaetognaths and fish larvae between the surface and the intermediate level.

Fish larvae abundances ranged from 1 to 170 individuals per 1000 m^3 . As with the other zooplankton, there were statistically significant differences ($P < 0.01$) (Table 1) between O_2 isopleths at all the stations (Fig. 4b), with the highest fish larvae abundance along the $100 \mu\text{mol kg}^{-1}$ in oxic conditions. Likewise, the greatest fish larvae concentrations were observed at the NW sampling stations in zones with relatively high CHL concentration (r.u.), as is the case of the zooplankton biomass.

From 700 fish larvae, identifications were made of 33 taxa (Table 3). Most of them were larvae of bathypelagic and mesopelagic fish, characteristic of this oceanic environment. The dominant taxa according to

Table 1

Mean abundance (ind 1000 m⁻³), standard deviation and coefficient of variation of the zooplankton groups collected in three different level depth in the oxygen minimum zone off southern Mexico (December 2020).

	Oxygenated			Below oxycline			Suboxic		
	Mean (n = 5)	Std. Deviation	Var. Coef	Mean (n = 5)	Std. Deviation	Var. Coef	Mean (n = 5)	Std. Deviation	Var. Coef
Copepods	33,709.1	52,935.0	1.6	3898.5	6311.4	1.6	559.0	350.7	0.6
Forams	3083.3	6568.9	2.1	22.4	18.1	0.8	8.6	6.0	0.7
Chaetognaths	2511.0	4488.5	1.8	17.7	17.5	1.0	13.5	7.7	0.6
Ostracods	828.6	1660.2	2.0	38.0	32.0	0.8	18.4	27.2	1.5
Echinoderms	669.6	1060.3	1.6	16.5	23.1	1.4	3.8	0.7	0.2
Pteropods	599.5	1211.0	2.0	18.2	13.6	0.7	5.7	3.5	0.6
Radiolarians	556.4	1073.9	1.9	123.9	197.1	1.6	19.3	14.4	0.7
Euphausiids	408.3	481.0	1.2	188.1	395.5	2.1	7.0	8.1	1.2
Siphonophores	364.3	509.0	1.4	31.4	26.5	0.8	6.5	4.1	0.6
Appendicularians	292.8	522.4	1.8	20.3	34.7	1.7	4.2	3.2	0.8
Amphipods	286.6	307.7	1.1	60.7	59.6	1.0	27.0	26.2	1.0
Heteropods	166.2	337.2	2.0	3.1	1.9	0.6	0.7	0.4	0.6
Leucifer	144.7	282.8	2.0	1.2	1.7	1.4	0.1	0.2	2.2
Decapods	143.1	296.3	2.1	1.3	2.7	2.1			
Annelids	128.6	224.7	1.7	51.0	67.9	1.3	3.3	4.5	1.4
Fish larvae	114.4	39.4	0.3	3.6	7.3	2.1	1.1	1.8	1.6
Cladocerans	88.1	140.0	1.6	0.2	0.5	2.2	0.4	0.4	1.1
Gastropods	63.0	126.1	2.0	0.9	1.1	1.2			
Bivalves	38.5	86.0	2.2				0.1	0.2	2.2
Thaliaceans	36.3	47.0	1.3	2.1	2.0	1.0	1.3	1.1	0.8
Mysids	28.8	51.2	1.8						
Stomatopods	26.2	39.5	1.5	0.2	0.4	1.5			
Jellyfish	19.2	43.0	2.2	0.5	0.7	1.4	0.1	0.2	2.2
Cirripedians	15.0	31.9	2.1	0.4	0.9	2.2	0.3	0.6	2.2
Cephalopod paralarvae	7.1	5.9	0.8	0.1	0.3	2.2			
Actinarian (anthozoans)	2.6	5.7	2.2						
Phyllosoma larvae	0.2	0.4	2.2						
Langoustines				0.1	0.3	2.2			

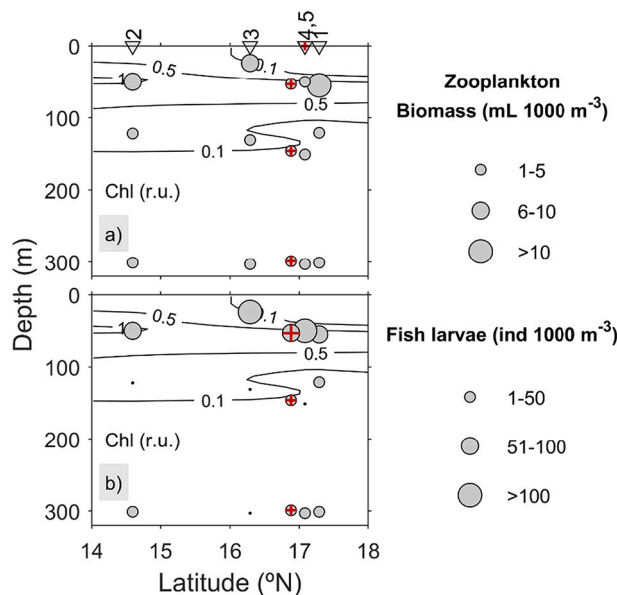


Fig. 4. Vertical distribution of zooplankton biomass (mL 1000 m⁻³) and fish larvae (ind 1000 m⁻³) along section in the oxygen minimum zone off southern Mexico (December 2020). Grey dots, biomass or abundance collected during night, and grey dots with red cross, biomass or abundance collected during the day. Isopleths represent chlorophyll a (r.u.). (For interpretation of the references to colour in this figure legend, the reader is referred to the web version of this article.)

Olmeasted-Tukey Test were *V. lucetia*, *D. laternatus*, *Diaphus pacificus*, *Cubiceps pauciradiatus* and *Diplophos proximus*. The constant taxa were *Lampanyctus parvicauda*, *Scopelogadus bispinosus*, *Lestidiops ringens*, *Ctenogobius* sp. 1 and *Malacoosteidae* type 1.

Table 2

Kruskall-Wallis and Mann-Whitney paired difference statistical analysis of zooplankton biomass and zooplankton groups, including fish larvae, among three depth levels with different oxygen concentrations in the oxygen minimum zone off southern Mexico (December 2020).

	Kruskall-Wallis		Mann-Whitney paired difference (p-value)		
	H (chi2)	p-value	Suboxyc		Oxycline
			Oxycline	Oxygenated	Oxygenated
Biomass	11.58	0.003	0.01*	0.01*	0.03*
Copepods	9.26	0.009	0.06	0.01*	0.09
Chaetognaths	9.38	0.009	1	0.01*	0.01*
Ostracods	7.61	0.022	0.25	0.02*	0.06
Pteropods	8.42	0.014	0.14	0.01*	0.09
Euphausiids	7.74	0.021	0.29	0.01*	0.09
Appendicularians	7.87	0.019	0.46	0.01*	0.06
Amphipods	6.5	0.039	0.53	0.02*	0.09
Fish larvae	9.62	0.008	0.75	0.01*	0.01*

The vertical distribution of the dominant species is shown in the Fig. 6. The highest abundances were observed along of the 100 μmol kg⁻¹ oxypleth tows (warm and oxic layer), but the greatest fish larvae abundance overall was found at the NW station where the highly saline Transitional Water was also observed. Fish larvae of these species were not observed in the deeper tows, where the dissolved oxygen concentration was <4.4 μmol kg⁻¹, except for the presence of *D. pacificus* (Fig. 6c).

Canonical analysis showed that the first two axes explained 48.7% of the variance (Fig. 7 and Table 4). Temperature, dissolved oxygen and CHL concentration (r.u.) showed an inverse correlation with the salinity. The 100 μmol kg⁻¹ oxypleth hauls (grey triangles) were associated with the highest values of temperature and dissolved oxygen, with the exception of the northernmost station that was more closely linked with CHL (r.u.). The 44 μmol kg⁻¹ oxypleth hauls (dark squares) and 4.4

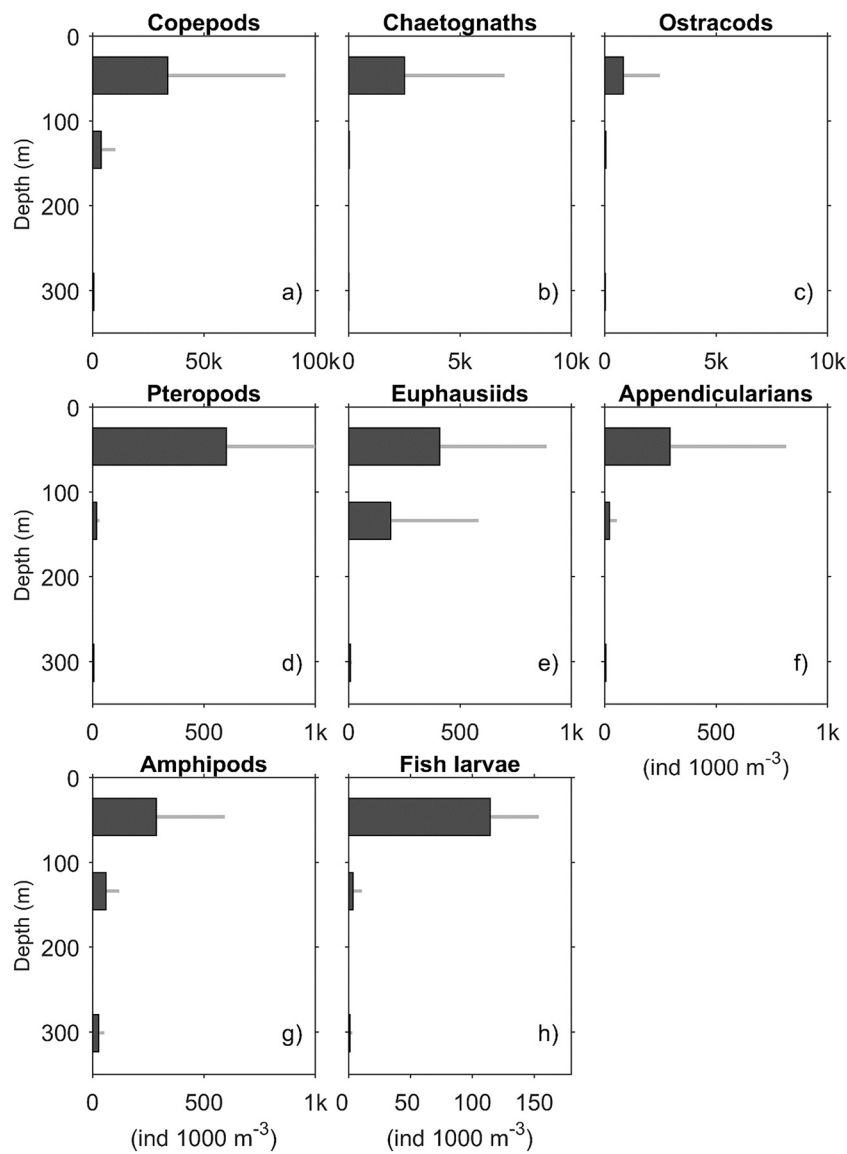


Fig. 5. Vertical distribution of the zooplankton groups ($\text{ind } 1000 \text{ m}^{-3}$) along section in the oxygen minimum zone off southern Mexico (December 2020). Mean abundance ($n = 5$). Grey line, standard deviation.

$\mu\text{mol kg}^{-1}$ oxypleth tows (dark triangles) were strongly associated with the highest salinity values and inversely associated with the other three variables, most strongly against dissolved oxygen.

The distribution of the zooplankton groups showed a preference for similar environmental conditions (Fig. 7). Most of the zooplankton groups showed their centroids around the cross of the axes, indicating that all variables contributed to their distribution. However, fish larvae were more closely associated with the highest values of temperature and dissolved oxygen.

4. Discussion

In this study, we investigated the relationships between the distribution of the zooplankton groups and the oceanographic conditions in the OMZ off southern Mexico, with an emphasis on the distributions of larval fish. Despite the reduced number of sampling locations, strong correlations were observed between zooplankton and dissolved oxygen in a previously poorly studied area of the largest OMZ on the planet.

The oceanographic conditions captured in the hydrographic section showed a confluence of water masses, where the Transitional Water was located on the NW side and the Tropical Surface Water on the SE (Figs. 2

and 3). Both surface water masses have been reported as characteristic of the region by Portela et al. (2016). The Tropical Surface Water was marked by a surface salinity minimum (Fig. 3b), even though previous authors have used low salinity as characteristic of the Tropical Branch of the California Current off Mexico (León-Chávez et al., 2010; Portela et al., 2018). This designation is based on the high temperature values ($>25^\circ\text{C}$) and remoteness of the study area from the Tropical Branch of California Current and the intervening higher salinities of the Transitional Water. Nevertheless, we recommend a future study to focus on the complex surface hydrography of this transitional region of the OMZ.

Below these surface water masses was the Subtropical Subsurface Water, characterized by oxygen deficiency (e.g., Chávez et al., 2003; Prince and Goodyear, 2006; Stramma et al., 2010). The vertical section of dissolved oxygen (Fig. 3c) shows that the $100 \mu\text{mol kg}^{-1}$ oxypleth (oxic conditions) was $\sim 60 \text{ m}$ depth and that the $44 \mu\text{mol kg}^{-1}$ oxypleth (hypoxic conditions), relatively close to the oxycline and the $100 \mu\text{mol kg}^{-1}$ oxypleth ($\sim 70 \text{ m}$ depth). We also note that the $4.4 \mu\text{mol kg}^{-1}$ oxypleth (suboxic conditions) rose from the NW ($\sim 150 \text{ m}$) to SE ($\sim 90 \text{ m}$), such that the hypoxic layer drastically thinned and the oxycline sharpened below the Tropical Surface Water area. This extreme shoaling of the suboxic water has previously been recorded only in coastal

Table 3

Characterization of the fish larvae assemblage using an Olmstead-Tukey Test in the oxygen minimum zone off southern Mexico (December 2020). D, dominant species; C, constant species; and R, rare species.

Species	Mean bundance	Standard deviation	Frequency of appearance (%)	Olmstead- Tukey Test
<i>Vinciguerria lucetia</i>	20.28	34.6	46.7	D
<i>Diogenichthys laternatus</i>	5.44	16.6	26.7	D
<i>Diaphus pacificus</i>	5.37	10.6	40.0	D
<i>Cubiceps pauciradiatus</i>	2.18	4.7	26.7	D
<i>Diplophos proximus</i>	1.19	2.8	33.3	D
<i>Lampanyctus parvicauda</i>	0.81	1.5	33.3	C
<i>Scopelogadus bispinosus</i>	0.36	1.0	20.0	C
<i>Lestidiops ringens</i>	0.31	0.8	20.0	C
<i>Ctenogobius</i> sp. 1	0.27	0.6	20.0	C
Malacosteidae type 1	0.25	0.4	26.7	C
<i>Scopelarchus</i> sp. 1	0.35	1.1	13.3	R
<i>Hyporhamphus rosae</i>	0.43	1.1	13.3	R
<i>Melanlagus bericoides</i>	0.26	0.7	13.3	R
<i>Penes pellucidus</i>	0.21	0.6	13.3	R
<i>Bathyllagooides wesethi</i>	0.20	0.6	13.3	R
<i>Acanthocybium solandri</i>	0.16	0.6	6.7	R
<i>Auxis</i> spp.	0.15	0.4	13.3	R
<i>Ctenogobius</i> sp. 2	0.14	0.5	6.7	R
<i>Etropus crossotus</i>	0.13	0.4	13.3	R
<i>Scopelarchoides nicholsi</i>	0.12	0.3	13.3	R
<i>Bolinichthys longipes</i>	0.11	0.4	6.7	R
<i>Bregmaceros</i> sp. 1	0.10	0.4	6.7	R
<i>Gempylus serpens</i>	0.10	0.4	6.7	R
Malacosteidae type 2	0.10	0.4	6.7	R
<i>Lestidiops</i> sp. 1	0.08	0.3	6.7	R
<i>Poromitra megalops</i>	0.07	0.2	13.3	R
<i>Idiacanthus antrostomus</i>	0.07	0.3	6.7	R
<i>Xyrichthys</i> sp. 1	0.07	0.3	6.7	R
<i>Eleotris picta</i>	0.06	0.2	6.7	R
<i>Bregmaceros bathymaster</i>	0.06	0.2	13.3	R
<i>Chiasonodon niger</i>	0.05	0.2	6.7	R
Congridae type 1	0.05	0.2	6.7	R
<i>Gonostoma</i> sp. 1	0.05	0.2	6.7	R
<i>Lampanyctus bristori</i>	0.05	0.2	6.7	R
Scombridae type 1	0.05	0.2	6.7	R
<i>Hygophum atratum</i>	0.01	0.0	6.7	R

upwelling areas in the northern area of the OMZ off Mexico (León-Chávez et al., 2015; Sánchez-Velasco et al., 2019; Trucco-Pignata et al., 2019). Even though the ocean is highly variable due to the different spatial and temporal oceanographic processes that act simultaneously, the results of this study provide insight into the impact of future vertical expansion of suboxic water in the OMZ on zooplankton that are highly sensitive to environmental changes (e.g., Diaz and Rosenberg, 2008; Gallo and Levin, 2016).

We observed that the highest zooplankton biomass, and most of the copepods, chaetognaths, ostracods, euphausiids, and total fish larvae resided in warm and oxic conditions, showing statistically significant differences ($P < 0.01$) with the deeper levels (Figs. 5 and 7), which were

almost empty. These results agree with Wishner et al.'s (2013, 2018) observations in the Tehuantepec Basin and Costa Rica Dome, who found zooplankton biomass to decrease drastically in the core of the OMZ, where dissolved oxygen concentrations reach $<4.4 \mu\text{mol kg}^{-1}$ independent of the depth. However, our results and those of Wishner et al. (2013, 2018), contrast with the findings of Longhurst (1985), who described that even though the zooplankton organisms were more concentrated in the euphotic zone in the Costa Rica Dome, they were also present until 300 m depth, the deepest stratum studied here.

An important difference between the Longhurst study and ours was the vertical distribution of the dissolved oxygen. Longhurst found dissolved oxygen concentrations $>44 \mu\text{mol kg}^{-1}$ ($>1 \text{ mL L}$) from ~ 110 m depth to surface, while we found this oxypleth at ~ 70 m depth. This could be the limiting factor in the zooplankton distribution below Tropical Surface Water, where the suboxic conditions were detected ~ 100 m depth. The shoaling of the suboxic water to the oxic layer implies the disappearance of the physiological buffer zone of zooplankton that exhibit vertical migrations to below the oxycline to avoid predation. Previous authors like Sánchez-Velasco et al. (2019) described the thinning of the hypoxic layer, the physiological buffer zone of zooplanktonic organisms, in the entrance of the Gulf of California, suggesting that the organisms utilizing and relying on the hypoxic layer will be the first organisms affected by the deoxygenation of the oceans. Studies made in the Tehuantepec Basin and Costa Rica Dome (Wishner et al., 2013, 2018, 2020; Maas et al., 2014) also described and postulated decrement of the hypoxic layer with effects on the zooplankton vertical migration, although it should be noted that they used a smaller mesh size, and a different space-time scale than in this study.

Latitudinally, the fish larvae presented an abundance gradient that decreased from Transitional Water in the NW to Tropical Surface Water in the SE. Larvae of the dominant fish species as the bathypelagic *V. lucetia*, *D. laternatus* and *C. pauciradiatus* were present only in the warm and oxic tows in the Transitional Water and noticeably absent in the Tropical Surface Water where shallower suboxic conditions were found (Fig. 6), except for the *D. pacificus* larvae. The vertical distribution of some of these species contrasts with the previous records in the entrance of the Gulf of California, where species as *D. laternatus*, and to a lesser extent *V. lucetia*, are distributed vertically throughout the water column and through different dissolved oxygen conditions (Davies et al., 2015; Sánchez-Velasco et al., 2017; Sánchez-Velasco et al., 2019; Gutiérrez-Bravo et al., 2021). A possible explanation might be the mesoscale influence in the mouth of the Gulf of California and adjacent Pacific Ocean. High mesoscale activity is produced by the interaction of the Mexican Coastal Current and the projections of the coast that generate eddies that mix the water column and transport coastal water to the gulf mouth, as mentioned in Lavín et al. (2006) and Kurczyn et al. (2012). Those conditions were not present in our study, or at least at the time of the samplings.

The CHL satellite image (Fig. 1b) show that our study area was oligotrophic, but the CHL increased in an eddy observed in the SE of the transect. The CHL concentration (r.u.) along the section was relatively homogenous ($> 0.5 \text{ r. u.}$) (Fig. 3d), indicating that this variable was not a determinant on the latitudinal distribution of the fish larvae between the Transitional and Tropical Surface Water. Instead, the shoaling of the suboxic water below the Tropical Surface Water of the SE was likely the primary determinant of the distribution of larval fish. There have been studies in the OMZ that have explored the physical and chemical phenomena that are acting on the distribution of zooplankton and fish larvae. Our data indicate that deoxygenation has critical effects on the holoplanktonic organisms which is even more strongly evident in meroplankton organisms such as fish larvae, which temporarily live as zooplankton. Consequently, there may be less opportunity for these organisms to develop adaptations to low dissolved oxygen concentrations. This last idea must be a hypothesis to evaluate in future multidisciplinary studies.

However, dissolved oxygen concentration and other

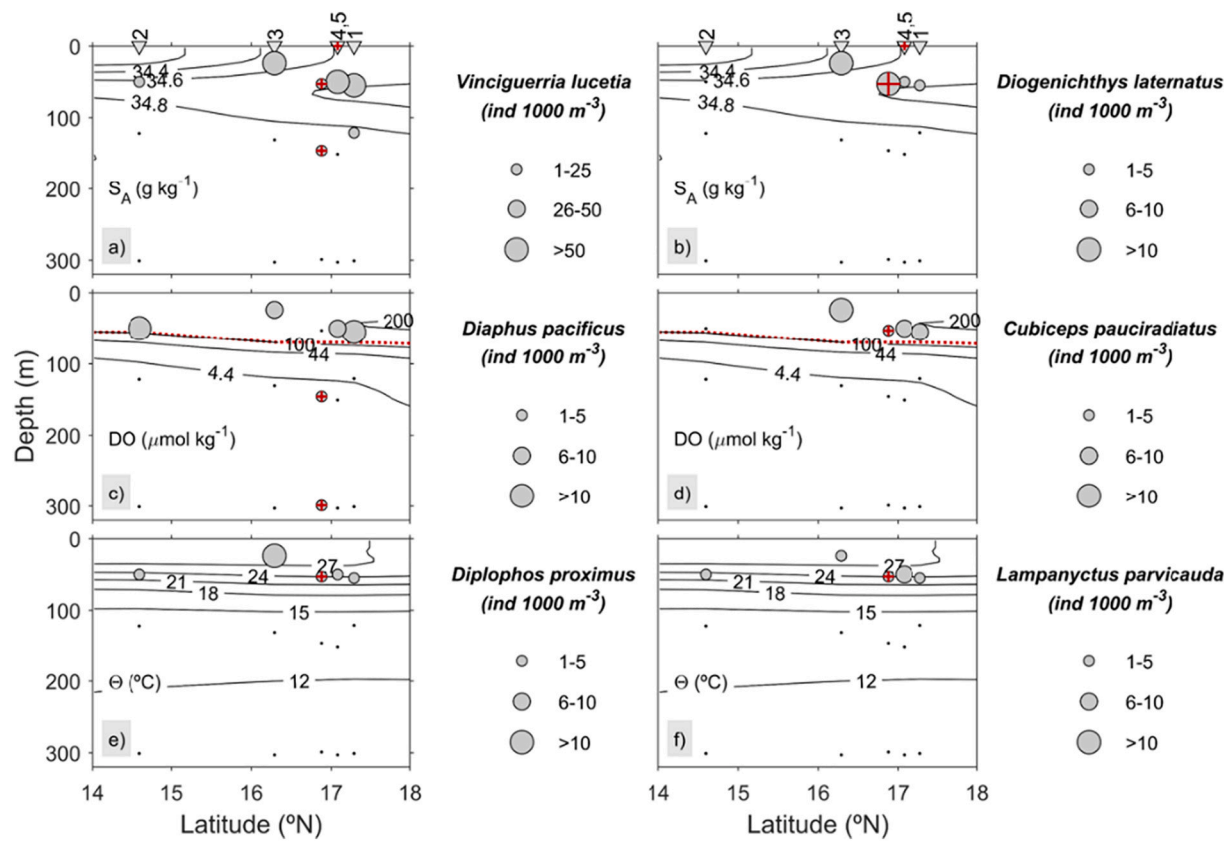


Fig. 6. Vertical distribution of the larvae of fish species (ind 1000 m⁻³) along section in the oxygen minimum zone off southern Mexico (December 2020). Grey dots, fish larvae collected during night, and grey dots with red cross, fish larvae collected during the day. Isopleths represent: a) and b) absolute salinity (S_A, g kg⁻¹), c) and d) dissolved oxygen (DO, µmol kg⁻¹) where the red line represents the oxycline, and e) and f) conservative temperature (Θ, °C). (For interpretation of the references to colour in this figure legend, the reader is referred to the web version of this article.)

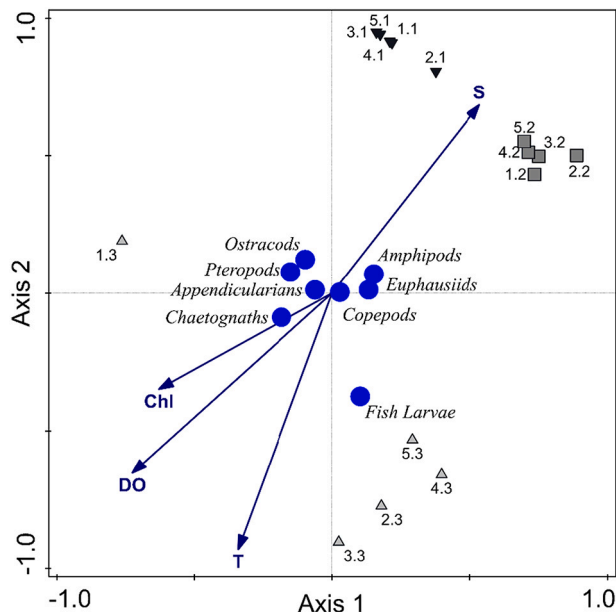


Fig. 7. Canonical correspondence analysis of zooplankton groups and environmental variables collected in the oxygen minimum zone off southern Mexico (December 2020). S, Absolute Salinity (S_A, g kg⁻¹); DO, dissolved oxygen (µmol kg⁻¹); Chl, chlorophyll a (u.r.); T, Conservative Temperature (Θ, °C). Grey triangles, 100 µmol kg⁻¹ oxypleth tows; dark squares, 44 µmol kg⁻¹ oxypleth tows; and dark triangles, 4.4 µmol kg⁻¹ oxypleth.

Table 4

Eigenvalues and explained variation between zooplankton groups and environment from the canonical correspondence analysis in the oxygen minimum zone off southern Mexico (December 2020).

Statistic	Axis 1	Axis 2	Axis 3	Axis 4
Eigenvalues	0.0274	0.02	0.0033	0.0017
Explained variation (cumulative)	17.84	30.88	33.03	34.13
Pseudo-canonical correlation	0.9011	0.9154	0.2577	0.2694
Explained fitted variation (cumulative)	52.26	90.47	96.77	100

physicochemical variables vary with depth, so they could covary positively or negatively. Such a situation avoids establishing with statistical precision if, for example, deoxygenation or greater depth or both are the variables that determine the abundance of zooplankton. Experimental studies would be required as the knowledge of suboxic condition tolerance of fish larvae would help to test these hypotheses. Despite limited sampling, our experience in other Pacific regions allows us to hypothesize that suboxic condition is the limiting factor for zooplankton organisms.

Previous authors have alerted us to the expansion of the OMZ (Paulmier and Ruiz-Pino, 2009; Stramma et al., 2010; Schmidtko et al., 2017; Wishner et al., 2018; Oschlies et al., 2018; Sánchez-Pérez et al., 2021) and the resulting impact on marine biota. Despite raising this alarm, it has been difficult to obtain financial support for continuing with regular zooplankton monitoring, which might give insight into the changes in the life cycles of pelagic organisms. Adapting fisheries plans, and limits of marine protected areas in the OMZ are integral to avoid catastrophic scenarios. Therefore, any information is important as a proxy of the deoxygenation and its effects in the marine ecosystem.

Declaration of Competing Interest

None.

Data availability

Data will be made available on request.

Acknowledgments

This study was supported by NSF award 1851361 (Mark Altabet, PI). The authors thank Mason Schettig, John Calderwood, and Emilio Garcia-Robledo for their help in the MOCNESS operation, and to the crew of the R/V Sally Ride, Scripps Institution. E.D.R.A. Thanks to Sistema Nacional de Investigadores-CONACyT for the support of investigator assistant. Special thanks to the editor and anonymous reviewers, whose professionalism much improved this article.

Appendix A. Supplementary data

Supplementary data to this article can be found online at <https://doi.org/10.1016/j.jmarsys.2022.103801>.

References

Boltovskoy, D., 1981. *Atlas del zooplancton del Atlántico Sudoccidental y métodos de trabajo con el zooplancton marino*. In: Instituto Nacional de Investigación y Desarrollo Pesquero Mar del Plata.

Breitburg, D., Levin, L.A., Oschlies, A., Grégoire, M., Chavez, F.P., Conley, D.J., Garçon, V., Gilbert, D., Gutiérrez, D., Isensee, K., Jacinto, G.S., Limburg, K.E., Montes, I., Naqvi, S.W.A.A., Pitcher, G.C., Rabalais, N.N., Roman, M.R., Rose, K.A., Seibel, B.A., Telszewski, M., Yasuhara, M., Zhang, J., 2018. Declining oxygen in the global ocean and coastal waters. *Science* 359, eaam7240. <https://doi.org/10.1126/science.aam7240>.

Cepeda-Morales, J., Gaxiola-Castro, G., Beier, E., Godínez, V.M., 2013. The mechanisms involved in defining the northern boundary of the shallow oxygen minimum zone in the eastern tropical Pacific Ocean off Mexico. *Deep Sea Res. Part I Oceanogr. Res. Pap.* 76, 1–12. <https://doi.org/10.1016/j.dsr.2013.02.004>.

Chávez, F.P., Ryan, J., Lluch-Cota, S.E., Niñuen-C, M., 2003. From anchovies to sardines and back: Multidecadal change in the Pacific Ocean. *Science* 299, 217–221. <https://doi.org/10.1126/science.1075880>.

Daniel, W.W., 2008. *Biostatistics: A Foundation for Analysis in Health Sciences*. John Wiley, Hoboken, USA.

Davies, S.M., Sánchez-Velasco, L., Beier, E., Godínez, V.M., Barton, E.D., Tamayo, A., 2015. Three-dimensional distribution of larval fish habitats in the shallow oxygen minimum zone in the eastern tropical Pacific off Mexico. *Deep Sea Res. Part I Oceanogr. Res. Pap.* 101, 118–129. <https://doi.org/10.1016/j.dsr.2015.04.003>.

Díaz, R.J., Rosenberg, R., 2008. Spreading dead zones and consequences for marine ecosystems. *Science* 321, 926–929.

Fernandez-Alamo, M.A., Farber-Lorda, J., 2006. Zooplankton and the oceanography of the eastern tropical Pacific: a review. *Prog. Oceanogr.* 69, 318–359. <https://doi.org/10.1016/j.pocean.2006.03.008>.

Fiedler, P.C., Talley, L.D., 2006. Hydrography of the eastern tropical Pacific: a review. *Prog. Oceanogr.* 69, 143–180. <https://doi.org/10.1016/j.pocean.2006.03.008>.

Gallo, N.D., Levin, L.A., 2016. Fish ecology and evolution in the world's oxygen minimum zones and implications of ocean deoxygenation. In: *Adv. Mar. Biol.* 1st ed. Elsevier Ltd. <https://doi.org/10.1016/bs.amb.2016.04.001>.

Godínez, V.M., Beier, E., Lavín, M.F., Kurczyn, J.A., 2010. Circulation at the entrance of the Gulf of California from satellite altimeter and hydrographic observations. *J. Geophys. Res. Oceans* 115 <https://doi.org/10.1029/2009JC005705>.

Gómez-Valdivia, F., Parés-Sierra, A., Flores Morales, A.L., 2015. The Mexican Coastal Current: a subsurface seasonal bridge that connects the tropical and subtropical Northeastern Pacific. *Cont. Shelf Res.* 110, 100–107. <https://doi.org/10.1016/j.csr.2015.10.010>.

Gutiérrez-Bravo, J.G., Tenorio-Fernández, L., Jiménez-Rosenberg, S.P.A., Sánchez-Velasco, L., 2021. Three-dimensional distribution of larval fish habitats at the entrance of the Gulf of California in the tropical-subtropical convergence region off Mexico (April 2012). *J. Plankton Res.* 1 (1), 1–15. [10.1093/plankt/fbab085](https://doi.org/10.1093/plankt/fbab085).

IOC, SCOR, IAPSO, 2010. The international thermodynamic equation of seawater – 2010: Calculation and use of thermodynamic properties. In: *Intergovernmental Oceanographic Commission, Manuals and Guides No. 56*, UNESCO (English), p. 196.

Kessler, W.S., 2006. The circulation of the eastern tropical Pacific: a review. *Prog. Oceanogr.* 69, 181–217. <https://doi.org/10.1016/j.pocean.2006.03.008>.

Koslow, J.A., Goericke, R., Lara-Lopez, A., Watson, W., 2011. Impact of declining intermediate-water oxygen on deepwater fishes in the California Current. *Mar. Ecol. Prog. Ser.* 436, 207–218. <https://doi.org/10.3354/meps09270>.

Kramer, D., Kalin, M.J., Stevens, E.G., Thrailkill, J.R., Zweifel, J.R., 1972. Collection and processing data on fish eggs and larvae in the California Current region. NOAA Technical Report.

Kurczyn, J.A., Beier, E., Lavín, M.F., Chaigneau, A., 2012. Mesoscale eddies in the northeastern Pacific tropical-subtropical transition zone: statistical characterization from satellite altimetry. *J. Geophys. Res. Oceans* 117, C10021. <https://doi.org/10.1029/2012jc007970>.

Lavín, M.F., Beier, E., Gómez-Valdés, J., Godínez, V.M., García, J., 2006. On the summer poleward coastal current off SW Mexico. *Geophys. Res. Lett.* 33, L02601. <https://doi.org/10.1029/2005GL024686>.

León-Chávez, C.A., Sánchez-Velasco, L., Beier, E., Lavín, M.F., Godínez, V.M., Färber-Lorda, J., 2010. Larval fish assemblages and circulation in the Eastern Tropical Pacific in autumn and winter. *J. Plankton Res.* 32, 397–410. <https://doi.org/10.1093/plankt/fbp138>.

León-Chávez, C.A., Beier, E., Sánchez-Velasco, L., Barton, E.D., Godínez, V.M., 2015. Role of circulation scales and water mass distributions on larval fish habitats in the Eastern Tropical Pacific off Mexico. *J. Geophys. Res. Oceans* 120, 3987–4002. <https://doi.org/10.1002/2014JC010289>.

Levin, L.A., 2002. Deep-Ocean life where oxygen is scarce. *Am. Sci.* 90, 436–444. <https://doi.org/10.1511/2002.33.756>.

Longhurst, A.R., 1985. Relationship between diversity and the vertical structure of the upper ocean. *Deep-Sea Res.* 32, 1535–1570.

Maas, A.E., Frazer, S.L., Outram, D.M., Seibel, B.A., Wishner, K.F., 2014. Fine-scale vertical distribution of macroplankton and microneuston in the Eastern Tropical North Pacific in association with an oxygen minimum zone. *J. Plankton Res.* 36, 1557–1575. <https://doi.org/10.1093/plankt/fbu077>.

Moser, H.G., 1996. *The Early Stages of Fishes in the California Current Region*, 33. US Department of the Interior, Minerals Management Service, p. 1505.

Oschlies, A., Brandt, P., Stramma, L., Schmidtko, S., 2018. Drivers and mechanisms of ocean deoxygenation. *Nat. Geosci.* 11, 467–473. <https://doi.org/10.1038/s41561-018-0152-2>.

Palomares-García, R., Suárez-Morales, E., Hernández-Trujillo, S., 1998. *Catálogo de los copépodos (Crustacea) pelágicos del Pacífico Mexicano*. CICIMAR-Ecosur, p. 352.

Paulmier, A., Ruiz-Pino, D., 2009. Oxygen minimum zones (OMZs) in the modern ocean. *Prog. Oceanogr.* 80, 113–128. <https://doi.org/10.1016/j.pocean.2008.08.001>.

Pawlowicz, R., Wright, D.G., Miller, F.J., 2010. The effects of biogeochemical processes on oceanic conductivity/salinity/density relationships and the characterization of real seawater. *Ocean Sci. Discuss.* 7, 773–836.

Portela, E., Beier, E., Barton, E.D., Castro, R., Godínez, V.M., Palacios-Hernández, E., Fiedler, P.C., Sánchez-Velasco, L., Trasviña, A., 2016. Water masses and circulation in the Tropical Pacific off central Mexico and surrounding areas. *J. Phys. Oceanogr.* 46, 3069–3081. <https://doi.org/10.1175/JPO-D-16-0068.1>.

Portela, E., Beier, E., Barton, E.D., Sánchez-Velasco, L., 2018. Surface salinity balance in the Tropical Pacific Off Mexico. *J. Geophys. Res. Oceans* 123, 5763–5776. <https://doi.org/10.1029/2018JC014265>.

Prince, E.D., Goodyear, C.P., 2006. Hypoxia-based habitat compression of tropical pelagic fishes. *Fish. Oceanogr.* 15, 451–464. <https://doi.org/10.1111/j.1365-2419.2005.00393.x>.

Ruvalcaba-Aroche, E.D., Sánchez-Velasco, L., Beier, E., Godínez-Sandoval, V.M., Barton, E.D., 2020. Ommastrephid squid paralarvae distribution and transport under contrasting interannual conditions in the tropical-subtropical convergence off Mexico. *Deep Sea Res. Part I*, 1–13. <https://doi.org/10.1016/j.dsr.2020.103259>.

Sánchez-Pérez, E.D., Sánchez-Velasco, L., Ruvalcaba-Aroche, E.D., Ornelas-Vargas, A., Beier, E., Barton, E.D., Peña, M.A., Godínez, V.M., Contreras-Catala, F., 2021. Temperature and dissolved oxygen concentration in the Pacific Ocean at the northern region of the oxygen minimum zone off Mexico between the last two PDO cool phases. *J. Mar. Syst.* 222, 103607 <https://doi.org/10.1016/j.jmarsys.2021.103607>.

Sánchez-Velasco, L., Beier, E., Godínez, V.M., Barton, E.D., Santamaría-del-Ángel, E., Jiménez-Rosenberg, S.P.A., Marinone, S.G., 2017. Hydrographic and fish larvae distribution during the “Godzilla El Niño 2015–2016” in the northern end of the shallow oxygen minimum zone of the Eastern Tropical Pacific Ocean. *J. Geophys. Res. Oceans* 122 <https://doi.org/10.1002/2016JC012622> n/a-n/a.

Sánchez-Velasco, L., Godínez, V.M., Ruvalcaba-Aroche, E.D., Márquez-Artavia, A., Beier, E., Barton, E.D., Jiménez-Rosenberg, S.P.A., 2019. Larval fish habitats and deoxygenation in the northern limit of the oxygen minimum Zone off Mexico. *J. Geophys. Res. Oceans* 124, 9690–9705. <https://doi.org/10.1029/2019JC015414>.

Schmidtko, S., Stramma, L., Visbeck, M., 2017. Decline in global oceanic oxygen content during the past five decades. *Nature* 542, 335–339. <https://doi.org/10.1038/nature21399>.

Smith, P.E., Richardson, S.L., 1979. *Técnicas Modelo Para Prospecciones de Huevos y Larvas de Peces Pelágicos*. FAO Doc. Tec. Pesca, p. 175.

Sokal, R.R., Rohlf, F.J., 1985. *Biometry*. Blume, Barcelona, Spain, p. 587.

Stramma, L., Johnson, G.C., Sprintall, J., Mohrholz, V., 2008. Expanding Oxygen-Minimum Zones in the Tropical Oceans. *Science* 320, 655–658. <https://doi.org/10.1126/science.1153847>.

Stramma, L., Schmidtko, S., Levin, L.A., Johnson, G.C., 2010. Ocean oxygen minima expansions and their biological impacts. *Deep Sea Res. Part I. Oceanogr. Res. Papers* 57, 587–595.

Suárez-Morales, E., Franco-Gordo, C., Suárez-Lozano, M., 2000. On the pelagic copepod community of central mexican tropical Pacific (Autumn, 1990). *Crustaceana* 73, 751–761.

Ter Braak, C.J.F., 1986. Canonical correspondence analysis: a new eigenvector technique for multivariate direct gradient analysis. *Ecology* 67, 1167–1179.

Trucco-Pignata, P.N., Hernández-Ayón, J.M., Santamaría-del-Ángel, E., Beier, E., Sánchez-Velasco, L., Godínez, V.M., Norzagaray, O., 2019. Ventilation of the Upper

Oxygen Minimum Zone in the Coastal Region Off Mexico: Implications of El Niño 2015–2016. *Front. Mar. Sci.* 6, 459. <https://doi.org/10.3389/fmars.2019.00459>.

Wiebe, P.H., Flierl, G.R., Davis, C.S., Barber, V., Boyd, S.H., 1985a. Macrozooplankton biomass in Gulf Stream warm-core rings: spatial distribution and temporal changes. *J. Geophys. Res. Oceans.* 90, 8885–8901.

Wiebe, P.H., Morton, A.W., Bradley, A.M., Backus, R.H., Craddock, J.E., Barber, V., Cowles, T.J., Flierl, G.R., 1985b. New development in the MOCNESS, an apparatus for sampling zooplankton and microneuston. *Mar. Biol.* 87, 313–323. <https://doi.org/10.1007/BF00397811>.

Wishner, K.F., Outram, D., Seibel, B.A., Daly, K.L., Williams, R.L., 2013. Zooplankton in the eastern tropical north Pacific: boundary effects of oxygen minimum zone expansion. *Deep-Sea Res. I Oceanogr. Res. Pap.* 79, 122–140. <https://doi.org/10.1016/j.dsr.2013.05.012>.

Wishner, K.F., Seibel, B.A., Roman, C., Deutsch, C., Outram, D., Shaw, C.T., Birk, M.A., Mislan, K.A.S., Adams, T.J., Moore, D., Riley, S., 2018. Ocean deoxygenation and zooplankton: very small oxygen differences matter. *Sci. Adv.* 4, 1–8.

Wishner, K.F., Seibel, B., Outram, D., 2020. Ocean deoxygenation and copepods: coping with oxygen minimum zone variability. *Biogeosciences* 17, 2315–2339. <https://doi.org/10.5194/bg-17-2315-2020>.

Wyrtki, K., 1966. Oceanography of the eastern equatorial Pacific Ocean. *Oceanogr. Mar. Biol. Annu. Rev.* 4, 33–68.